Food Control 115 (2020) 107278

Contents lists available at ScienceDirect

Food Control

journal homepage: www.elsevier.com/locate/foodcont

Antimicrobial kinetics of nisin and grape seed extract against inoculated *Listeria monocytogenes* on cooked shrimps: Survival and residual effects

Xue Zhao[a,b], Lin Chen[a,b], Lin Zhao[a,b], Yun He[a,b], Hongshun Yang[a,b,*]

[a] Department of Food Science & Technology, National University of Singapore, Singapore, 117542, Singapore
[b] National University of Singapore (Suzhou) Research Institute, 377 Lin Quan Street, Suzhou Industrial Park, Suzhou, Jiangsu, 215123, PR China

ARTICLE INFO

Keywords:
Listeria monocytogenes
Nisin
Natural extract
Ready-to-eat food
Modelling
Atomic force microscopy
Seafood
Nanostructure
Microbial safety
Inactivation
Antimicrobial agent
Mechanism
Color
Storage
Kinetics
Foodborne pathogen
Preservation
Aquatic food
Morphology

ABSTRACT

The antimicrobial effects of nisin (2000 IU/mL) and grape seed extract (GSE, 1%) against *Listeria monocytogenes* (SSA184, SSA97 and LM10) inoculated on cooked shrimps (*Litopenaeus vannamei*) were investigated. Notable reductions (1.7–1.9 log CFU/g reduction) of *L. monocytogenes* were observed after 15-min treatment of combined nisin and GSE while SSA184 showed the highest susceptibility to the activity of nisin and GSE as compared to other strains. The atomic force microscopy results indicated that greater morphological changes were found in combination treated cells of SSA184, whose width (0.47 μm) and height (0.25 μm) were decreased while the surface roughness (10.12 nm) was increased significantly ($P < 0.05$). Residual nisin and GSE further inhibited the listerial growth during storage (0.4–0.8 log CFU/g increment). Based on the fitting goodness, Weibull and Baranyi models were verified as the best ones to describe inactivation kinetics of *L. monocytogenes* and growth dynamics during storage, respectively. Additionally, the colour of cooked shrimpsafter combined treatment were not negatively affected and even protected during storage. In conclusion, the antimicrobial treatment of combined nisin and GSE could be a potential antilisterial strategy for shrimps.

1. Introduction

Consumer demand for safe and fresh seafood and seafood products has attracted increasing interest in recent decades because of their health-benefits. Nevertheless, seafood products are highly perishable under microbial activities, resulting in non-negligible bacterial contamination. Such adverse contaminations usually occur during cultivating, processing, transporting and storage (Vongkamjan, Benjakul, Vu, & Vuddhakul, 2017). Bacterial contaminants can cause spoilage when the microbial populations exceed 6–7 log colony forming unit (CFU)/g and further result in undesirable odours and tastes (Semeano et al., 2018). However, seafood has been a primary product responsible for foodborne outbreaks in Singapore and other coastal regions. Pathogenic microorganisms of major concerns in seafood include *Salmonella*, *Vibrio* spp., and *Listeria monocytogenes*. It is of great concern as *L. monocytogenes* can survive and multiply in seafood matrix which are stored under low temperature and induce severe foodborne illness and even death (Afari & Hung, 2018). It has been reported that shrimp, especially ready-to-eat shrimp (i.e., cooked shrimp) has high potential for *L. monocytogenes* contamination (Elbashir et al., 2018). Thus, a promising antimicrobial strategy is needed to control the listerial contamination on shrimp.

Nisin, a natural, low molecular, and hydrophobic peptide with 34 amino acid residues, is mainly produced by some *Lactococcus lactis* strains (Ayyash et al., 2019; Bekhit, Sánchez-González, Messaoud, & Desobry, 2016). As a broad spectrum bacteriocin, nisin exhibits inactivation effect against a wide broad of Gram-positive foodborne pathogens as well as spore-producing bacteria, for example *L. monocytogenes* and *Staphylococcus aureus* (Morsy, Elsabagh, & Trinetta, 2018; Zhao et al., 2014). Nisin has been approved for application in food as a safe antimicrobial agent by the Food and Agriculture Organisation (FAO)/World Health Organisation (WHO) Committee on Food

* Corresponding author. Department of Food Science & Technology National University of Singapore, Singapore, 117542, Singapore.
E-mail address: fstynghs@nus.edu.sg (H. Yang).

https://doi.org/10.1016/j.foodcont.2020.107278
Received 5 February 2020; Received in revised form 24 March 2020; Accepted 26 March 2020
Available online 31 March 2020
0956-7135/ © 2020 Elsevier Ltd. All rights reserved.

Abbreviations

CFU	colony forming unit
FAO	Food and Agriculture Organisation
WHO	World Health Organisation
GRAS	generally recognised as safe
GSE	grape seed extract
SEM	scanning electron microscopy
TEM	transmission electron microscopy
AFM	atomic force microscopy
DI	deionised
TSB	tryptone soya broth
TSA	tryptone soya agar
PBS	phosphate buffer saline
HCl	hydrochloric acid
SSE	Sum of Squares for Error
RMSE	Root Mean Squared Error
AIC	Akaike Information Criterion
BIC	Bayesian Information Criterion
Af	accuracy factor
Bf	bias factor
D%	discrepancy percentage
B%	bias percentage
RMS	root-mean-square
ANOVA	analysis of variance
LSD	least significant difference
CEO	cinnamon essential oil
REO	rosemary essential oil

Additives and Ingredients and obtained a generally recognised as safe (GRAS) status by Food and Drug Administration (Hanušová et al., 2010). Due to the high level of safety and sterilisation rate, nisin has been applied for preservation of seafood, such as chilled vacuum packed tuna and gilthead seabream, and has been reported as an efficient anti-listerial material (Shi et al., 2017; Sofra, Tsironi, & Taoukis, 2018). However, nisin shows limited antimicrobial effect against Gram-negative bacteria, and its antimicrobial activity as well as solubility are related to low pH condition, and the stability decreases during storage (Ibarra-Sánchez, Van Tassell, & Miller, 2018). Thus, it is of great significance to increase its stability and antimicrobial ability, as well as to broaden its application. Combination of nisin with other antimicrobial agents may be a promising method. For example, nisin-based tertiary antimicrobial mixtures preserved the overall quality of refrigerated Argentine hake to 30 days and inhibited growth of *L. monocytogenes* during refrigeration (Schelegueda, Delcarlo, Gliemmo, & Campos, 2016).

Grape seed extract (GSE) is a plant derived additive that generated with a considerable quantity during wine production. Similar to nisin, GSE is verified as a GRAS food additive (Zhao, Wu, Chen, & Yang, 2019a). Due to its abundant contents of polyphenols like proanthocyanidins, GSE is proved to have strong antioxidant ability (Chen et al., 2018; Haskaraca, Juneja, Mukhopadhyay, & Kolsarici, 2019). It has been applied to different seafood such as silver carp and tilapia fillets to retard the lipid and protein oxidation (Shi, Cui, Yin, Luo, & Zhou, 2014; Zhao et al., 2019c). Moreover, GSE has drawn further attention because of its promising antimicrobial property. Recent studies have revealed the inactivation effeicacy of GSE against *L. monocytogenes*, *Bacillus cereus*, *S. aureus*, *Bacillus subtilis*, *Lactobacillus fermentum*, *Escherichia coli*, *Streptococcus thermophilus*, *Pseudomonas aeruginosa*, and *Lactobacillus vaginalis* (Tabasco et al., 2011).

The optical microscope is a useful tool for the observation of bacteria, but the resolution is limited by the wavelength of the light source. Scanning electron microscopy (SEM) and transmission electron microscopy (TEM) can provide high-resolution images of cells (Bergmans et al., 2015). Nevertheless, the sample preparation is complicated and vacuum condition could induce substantial distortion of cell structure. Atomic force microscopy (AFM) provides a new chance to study the surface characteristics of cells *in situ* at nanoscale level (Yang et al., 2007). It has gained its popularity recently as an important aid to traditional techniques for high-resolution imaging and microbiological analysis (Liu, Tan, Yang, & Wang, 2017). It is superior to SEM and TEM in some extent as it can provide 3-dimensional topological structure and conduct sample observation in aqueous condition, making it possible to real-time monitor surface properties of live cells and non-destructively test the membrane. AFM can also qualitatively probe the interaction based on the distance between tip and sample as well as the elasticity of bacteria (Liu & Yang, 2019).

The aim of this work was to evaluate the antimicrobial effects of nisin, GSE and their combination against inoculated *L. monocytogenes* on cooked shrimps. The antilisterial activity of nisin and GSE and their residual performance during 12-day storage (4 °C) were tested. The disinfection kinetics and model fitting test were conducted. Moreover, AFM was applied to monitor the cell morphological changes and thus preliminarily elucidate the underlying antimicrobial mechanism. Lastly, the effects of nisin and GSE on colour qualities of shrimps during storage were assessed.

2. Materials and methods

2.1. Chemicals and reagents

Deionised (DI) water was prepared using a Mill-Q purification system. Tryptone Soya Broth (TSB) and Tryptone Soya Agar (TSA) were purchased from (Oxoid, UK). Peptone water was purchased from Sigma-Aldrich (St, Louis, MO, USA). Phosphate buffer saline (PBS) was also obtained from Sigma-Aldrich. Nisin (2.5% balance sodium chloride) was purchased from Sigma-Aldrich (Singapore) while GSE was provided by Tianjin Jianfeng Natural Product Co., Ltd. (Tianjin, China). Analytical reagent grade hydrochloric acid (HCl, 37%) was purchased from Tokyo Chemical Industry Co., LTD (Tokyo, Japan).

The preparation of antimicrobial solutions was performed according to a method described by Zhao, Chen, Wu, He, and Yang (2020). The nisin stock solution (10^5 IU/mL) was prepared by dissolving 1 g nisin in 10 mL 0.02 M HCl. GSE was dissolved in sterile DI water using a stirrer. The combined nisin and GSE solution was obtained by mixing them at a ratio of 1:1 followed by stirring at room temperature thoroughly. The antimicrobial solutions were prepared using autoclaved DI water and were subject to filtration through a sterile syringe filter (0.22 μm) before use.

2.2. Bacterial strains and inoculum preparation

Three *L. monocytogenes* strains (SSA184 stereotype 3a, SSA97 stereotype 1/2b, and LM10 stereotype 4b) isolated from pre-paced smoked salmon were provided by the Environmental Health Institute of Singapore National Environment Agency (Yuan, Lee, & Yuk, 2017). The cryopreserved strains were activated in 5 mL TSB at 37 °C for 24 h. The working *L. monocytogenes* suspension was prepared by three successive inoculations in TSB (1:100) with an interval of 24 h (Jones & D'Orazio, 2013). The bacterial population was counted by plate culture on TSA. The *L. monocytogenes* suspension was centrifuged (12,000 × *g*, 10 min) and the harvest cell pellet was washed by PBS (0.1 M, pH 7.2) for three times. The *L. monocytogenes* inoculum was resuspended in 0.1% peptone water to reach a final level of 9 log CFU/mL (Zhao et al., 2020).

2.3. Inoculation and antimicrobial treatments of shrimps

Frozen cooked shrimps (*Litopenaeus vannamei*) were purchased from a local supermarket in Singapore. After thawing, shrimps were rinsed with sterile DI water. For microbial analysis, shrimps were treated with ultraviolet light in a biosafety cabinet (Esco Class II, Type A2, E-Series, Esco Micro Pvt. Ltd., Singapore) for 30 min (15 min on both sides) to remove background microflora. The inoculation of *L. monocytogenes* on shrimps was conducted by immerging into *L. monocytogenes* suspension for 5 min. The final concentration of *L. monocytogenes* on shrimps reached around 6 log CFU/g. The inoculated shrimps were air-dried for 10 min in a laminar flow BSC.

Inoculated samples were randomly divided and immersed in the following antimicrobial agents for 15 min at a ratio of 1:3 (w/v) respectively: (i) DI water (conducted as the control); (ii) nisin (2000 IU/mL); (iii) GSE (1%, w/v); (iv) the combination of nisin and GSE at a ratio of 1:1. Samples were taken at an interval of 1.5 min to allow for reliable kinetic analysis of microbial inactivation. The collected samples at different sampling times were immediately transferred to neutralising buffer (0.1 M PBS) for 1 min and then drained in a biosafety cabinet for 10 min. Lastly, the treated shrimps were kept in sterile bags and stored at 4 ± 1 °C up to 12 days. The populations of *L. monocytogenes* on shrimps during refrigeration were tested every three days.

2.4. Enumeration of L. monocytogenes

At each sampling time point, one piece of shrimp (10 ± 1.0 g) in each group was transferred to a stomacher bag containing 90 mL sterile peptone water (0.1%, w/v) for 3-min homogenisation (Masticator Stomacher, IUL Instruments, Germany). The samples were then decimally diluted by peptone water serially and 100 μL of diluent was plated on TSA plates. The colonies were counted after incubating at 37 °C for 2 days and expressed as log CFU/g sample (Jiang, Neetoo, & Chen, 2011).

2.5. Mathematical modelling of antibacterial effect

2.5.1. Model fitting

The antibacterial effect (log CFU/g reduction as compared to the initial population) of different treatments during inactivation process was described by the linear, Weibull, Huang's and Fermi models (Chen et al., 2020; Ghate et al., 2017). The residual antilisterial effect of each treatment during shrimp storage was described by the exponential, modified Gompertz, Beta function and Baranyi models (Dermesonluoglu et al., 2016; Ochoa-Velasco et al., 2018; Ye et al., 2013). Δy, y_0 and y in Equations 1–4 refer to the bacterial reduction (log CFU/g), the initial microbial load, and the population of bacteria surviving at treatment time x (min), respectively. In Equations 5–9, Δy is the bacterial increment (log CFU/g), y_0 is the initial microbial population (day 0, within 1 h after antimicrobial treatment), and y is the population of bacteria surviving at storage time x (day).

2.5.1.1. Linear model.

$$\Delta y = y_0 - y = ax + b \tag{1}$$

where a and b are the linear regression parameters.

2.5.1.2. Weibull model.

$$\Delta y = (x/c)^{\alpha} \tag{2}$$

where c is the time needed to achieve 1 log CFU/g reduction and α is the shape parameter.

2.5.1.3. Huang's model.

$$\Delta y = \beta\{x + 0.25\ln[(1 + e^{-4(x-\gamma)}/(1 + e^{4\gamma})]\} \tag{3}$$

where β is the maximum antibacterial rate and γ is lag phase duration (min).

2.5.1.4. Fermi model.

$$\Delta y = \log\left\{\frac{1 + \exp(-dxL)}{1 + \exp[d(x - xL)]}\right\} \tag{4}$$

where d is the maximum specific decay rate (log CFU/g/min) and xL is the time before inactivation.

2.5.1.5. Modified Gompertz model.

$$\Delta y = y - y_0 = A + C \times \exp\{-\exp[-B(x - M)]\} \tag{5}$$

where M is the time (day) at which the absolute rate of change is at a maximum level, B (log CFU/g/day) is the relative rate of change at time M, A is the value of the anterior variable (y) just at the beginning of the storage; C is the difference between the initial and last asymptotic values obtained for each variable during storage.

2.5.1.6. Exponential model.

$$\Delta y = \log[\exp(ux)] \tag{6}$$

where u is the general growth rate (log CFU/g/day).

2.5.1.7. Beta function.

$$\Delta y = Q\left(1 + \frac{x_Q - x}{x_Q - x_m}\right)\left(\frac{x}{x_Q}\right)^{\frac{x_Q}{x_Q - x_m}} \tag{7}$$

where Q is the maximum bacterial growth or death obtained at storage time x_Q (day) while x_m (day) is the time for the maximum growth rate.

2.5.1.8. Baranyi model.

$$\Delta y = \mu f(x) - \ln\left[1 + \frac{e^{\mu f(x)} - 1}{e^{(y_{max}')}}\right] \tag{8}$$

with

$$f(x) = x + \frac{1}{v}\ln[e^{-vx} + e^{-u\lambda} - e^{(vx-u\lambda)}] \tag{9}$$

where y_{max}' is the maximum increment of bacterial count during storage and μ is the specific growth rate (day^{-1}), v is the increase rate of the limiting substrate, assumed to the equal to μ while λ is the lag time (day).

To analyse the goodness of the model fitting, Sum of Squares for Error (SSE) as well as Root Mean Squared Error (RMSE) were calculated using MATLAB R2013b (The Mathworks Inc., Natick, MA, USA). Moreover, the Akaike Information Criterion (AIC) and Bayesian Information Criterion (BIC) values were used to determine the overfitting:

$$\mathrm{AIC} = n\ln(\mathrm{SSE}) + 2p \tag{10}$$

$$\mathrm{BIC} = n\ln(\mathrm{SSE}) + p\ln(n) \tag{11}$$

where n and p represent the number of data points and parameters used in each model, respectively (Ghate et al., 2017).

2.5.2. Model verification

Observed counts of *L. monocytogenes* (inactivation process: 7.5 min; storage: day 7) and predicted populations were compared by calculation of the validation indices Accuracy factor (A_f) and Bias factor (B_f):

$$A_f = \exp\left(\sqrt{\sum_{i=1}^{n}[\ln(u_{p,\,i}) - \ln(u_{o,\,i})]^2}\right) \tag{12}$$

$$B_f = \exp\left(\frac{\sum_{i=1}^{n} \ln(u_{p,\,i}) - \ln(u_{o,\,i})}{n}\right) \quad (13)$$

where u_p, u_o and n represent the predicted values from the selected model, observed values obtained from plate counting, and the number of observations, respectively (Ye et al., 2013). A perfect fitting is obtained when both A_f and B_f values reach 1.

The discrepancy percentage (D%) and bias percentage (B%) were determined by the following equations:

$$D\% = (A_f - 1) \times 100\% \quad (14)$$

$$B\% = \text{sgn}(\ln B_f) \times (\exp|\ln B_f| - 1) \times 100\% \quad (15)$$

where sgn ($\ln B_f$) equals to -1, 0 or 1 when B_f is negative, zero or positive, respectively. In general, positive and negative B% value indicate that the model predicts larger and smaller values as compared to the actual observed data, respectively. Higher the B% value, higher the value of underestimation or overestimation (Nyhan et al., 2018).

2.6. AFM analysis of morphological changes

AFM was conducted to monitor the changes in cell morphology of *L. monocytogenes* on shrimps by each treatment. The antimicrobial solutions containing shrimps after each treatment were transferred to a 50 mL sterile conical tube and centrifuged (500 × *g*, 1 min) to precipitate debris. The cells were then gained by centrifugation at high speed (12,000 × *g*, 10 min) and washed with 0.1M PBS for two times. After resuspending in PBS, 20 μL of *L. monocytogenes* suspension was spread onto a mica sheet and air-dried before analysis. The sheet of each treatment was imaged by AFM coupled with a Sensaprobe TM190-A-15 tip (Applied Nanostructures, Mountain View, CA, USA). The resonance, force constant, scan rate and line were set at 190 kHz, 45 N/m, 0.4 Hz and 512, respectively. The collected figures were processed by the offline software Gwyddion version 2.55. The width, height as well as root-mean-square (RMS) roughness of the listerial cells were determined (Chen et al., 2018).

2.7. Colour measurement

Colour changes of treated shrimps during chilled storage were evaluated using a Minolta Colorimeter CM-3500d (Konica Minolta, Tokyo, Japan) (Zhao, Zhao, Phey, & Yang, 2019b). The colour parameters, including L* (lightness), a* (redness-greenness), b* (blue-yellowness) were determined for each sample. Colour difference (ΔE) between fresh shrimp (untreated) and treated samples at each storage time was calculated using the following formula:

$$\Delta E = \sqrt{\Delta L^{*2} + \Delta a^{*2} + \Delta b^{*2}} \quad (16)$$

2.8. Statistical analysis

The analysis of variance (ANOVA) and the least significant difference (LSD) approach were conducted using IBM SPSS Statistics Version 23 (International Business Machines Co. Armonk, NY, USA) to evaluate the statistical differences among all experimental results. All experiments were performed at least three times independently. A P value < 0.05 was considered significantly different.

3. Results and discussion

3.1. Inhibitory effect of L. monocytogenes inoculated on shrimps

3.1.1. Antimicrobial activity of different treatments on L. monocytogenes

The inactivation effects on *L. monocytogenes* under different treatments are shown in Fig. 1A. The population of *L. monocytogenes* in the control group remained constant regardless of the strain type. *L. monocytogenes* SSA184 ranged from 6.1 to 6.5 log CFU/g during 15 min of treatment, whereas control SSA97 and LM10 fluctuated in the ranges of 5.8–6.0 and 6.0–6.2 CFU/g, respectively. Gradual reductions of *L. monocytogenes* on shrimps were observed after individual treatment of GSE, suggesting that all the strains were sensitive to this natural extract. Bisha, Weinsetel, Brehm-Stecher, and Mendonca (2010) also showed that a low concentration of GSE (0.125%) exhibited a prominent *in situ* antimicrobial effect on *L. monocytogenes* inoculated on Roma tomato

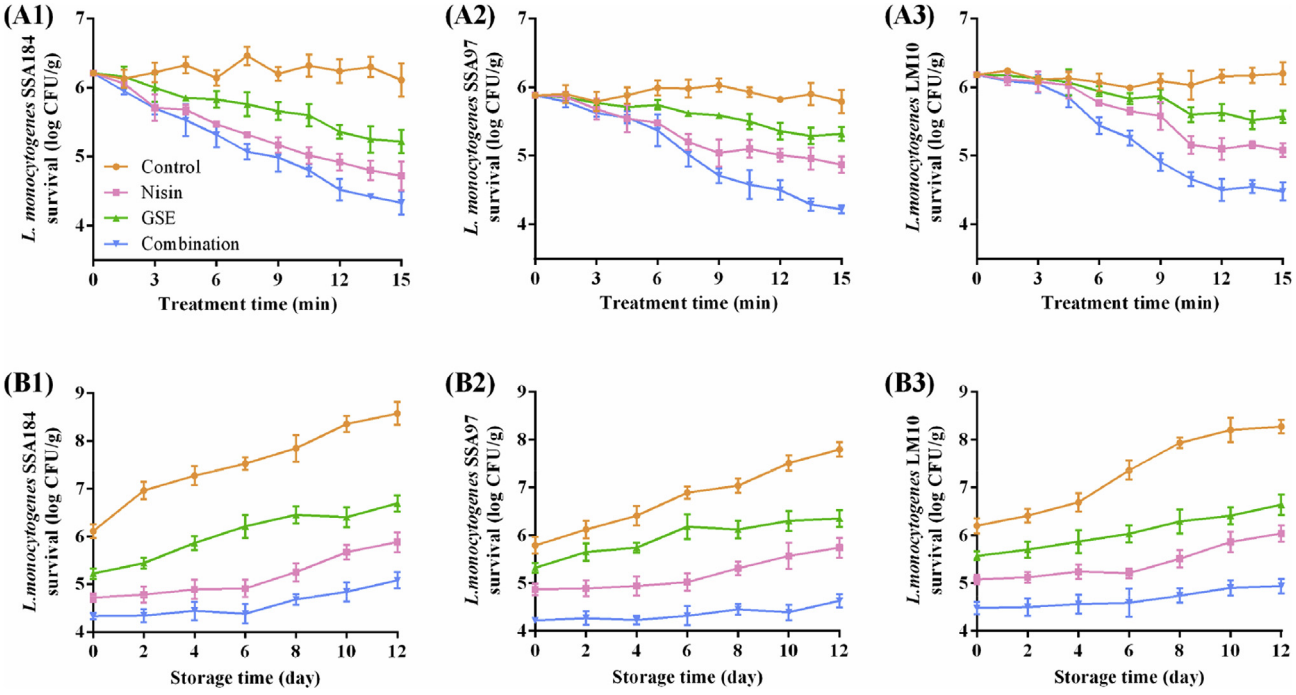

Fig. 1. Survival populations of inoculated *L. monocytogenes* on shrimps during inactivation (A) and storage (B) processes. Note: * the values on day 0 refer to the *L. monocytogenes* counts within 1h after antimicrobial treatments.

after 2 min of exposure. Single GSE treatment significantly reduced the SSA184 by 1.0 log CFU/g as compared to the corresponding control group ($P < 0.05$). The final log reductions of SSA97 and LM 10 were 0.5 and 0.6 log CFU/g, respectively, which were significantly lower than that of SSA184 reduction ($P < 0.05$). Similarly, nisin sharply reduced the *L. monocytogenes* counts by 1.0–1.5 log CFU/g and the highest listerial reduction were observed in the SSA184 strain. The results suggested that the *L. monocytogenes* SSA184 was more sensitive to both nisin and GSE treatments as compared to the other two *L. monocytogenes* strains. These findings are supported by previous studies which confirmed that the antimicrobial activity of phenolic compounds are strain-dependent and species-dependent (Fancello et al., 2020). The same polyphenol may be effective on one type of Gram-positive (or Gram-negative) bacteria and ineffective on the other ones, indicating species-dependent effect (Fancello et al., 2020). For example, epigallocatechin gallate was active against tested *L. monocytogenes* ATCC 19115 (100% reduction), *Pseudomonas aeruginosa* ATCC 27853 (74.7% reduction), *S. aureus* CNRZ3 (55.3% reduction) but exhibited a slight bacterial growth-inhibiting effect (17.7%) against *E. coli* ATCC 25922 (Bordes et al., 2019). Moreover, the antimicrobial ability of the same polyphenol was different among different strains. This is the case for example of procyanidins which exhibited a greater inhibitory effect against *S. aureus* CECT 976 than *S. aureus* CECT 4465 and CECT 828 (Alejo-Armijo et al., 2017). We thus postulate that the difference in bacterial sensitivity to the same polyphenol could related to the difference in cellular structure. In our study, GSE used was a mixture of polyphenols, which is composed of 80% procyanidin and some minor components (catechin, epicatechin, gallic acid, etc.). They worked

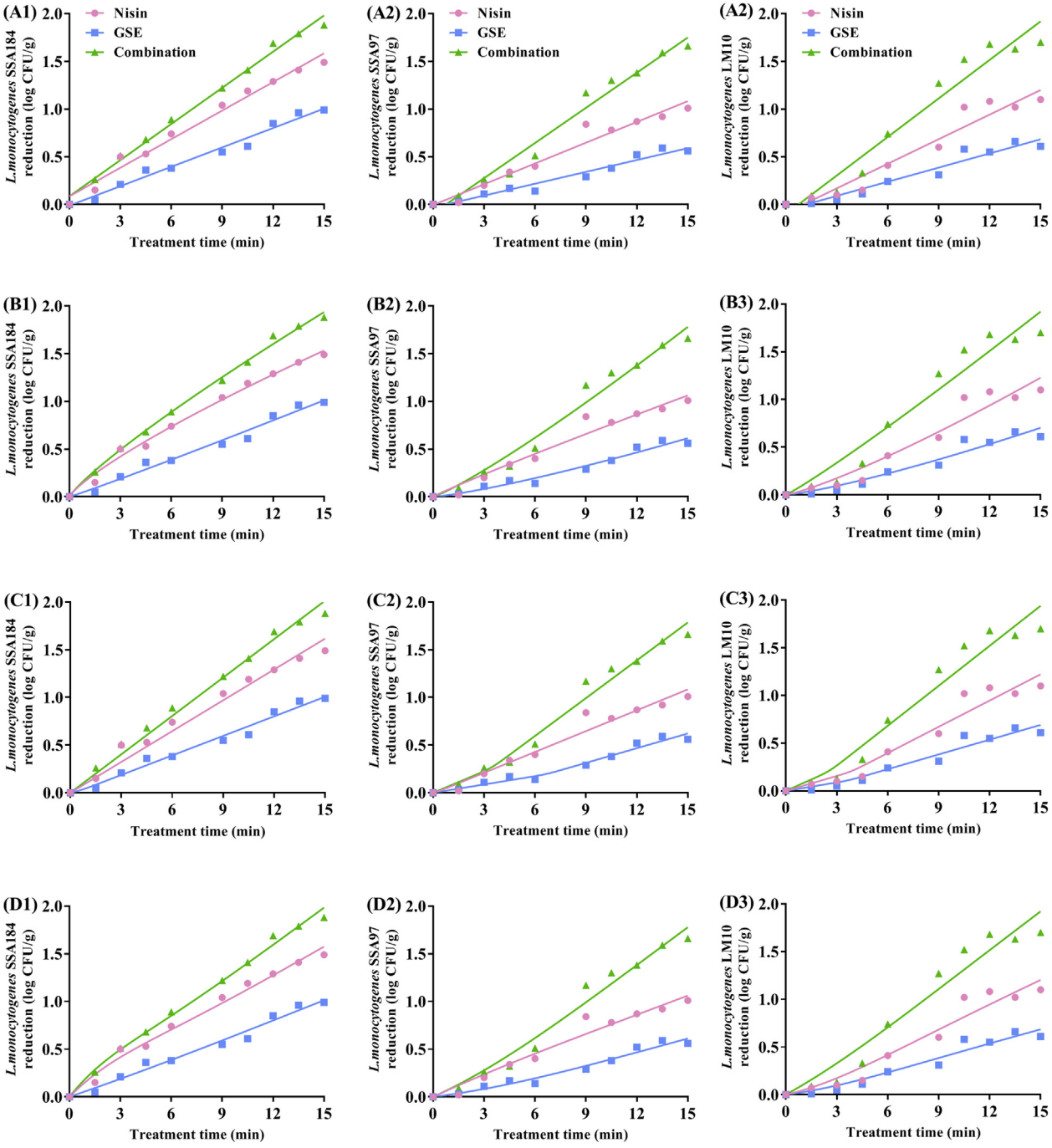

Fig. 2. Modelling of inoculated *L. monocytogenes* reduction on shrimps during inactivation process. (A) Linear, (B) Weibull, (C) Huang's and (D) Fermi models.

collectively to inactivate three tested *L. monocytogenes* strains, especially SSA184. On the other hand, strain differences in *L. monocytogenes* sensitivity to nisin, observed in our study, might be related to differences in phospholipid content, composition of membrane fatty acids and also the difficulty of nisin in forming pores in more solid membranes (Cotter, Guinane, & Hill, 2002; Solomakos, Govaris, Koidis, & Botsoglou, 2008). The strains with an increased ratio of straight-chain fatty acids as well as a lower ratio of branched-chain ones showed higher resistant against nisin. Moreover, the pore formation ability of nisin in *L. monocytogenes* membrane was related to the interaction between three positively charged lysine residues of nisin and anionic phospholipids. Therefore, the strains whose membrane were rigid due to the condensation of these phospholipids, such binary interaction was inhibited (Abee, 1995).

Furthermore, shrimps treated with combined nisin and GSE have the lowest final *L. monocytogenes* populations indicating an improved antimicrobial effect when applied in combination than in separate. Specifically, the counts of *L. monocytogenes* SSA184, SSA97 and LM10 remaining on shrimps after combined treatment were 4.3, 4.2 and 4.5 log CFU/g, respectively, with log differences of 1.9, 1.6 and 1.7 as compared to the respective control samples. Previous reports have verified the synergetic inactivation efficacy of combined sterilising agents (Raeisi, Tabaraei, Hashemi, & Behnampour, 2016; Xu et al., 2007). Raeisi et al., (2016) conducted an experiment to test the antimicrobial effects of nisin, cinnamon essential oil (CEO) and rosemary essential oil (REO) on inoculated *L. monocytogenes* on chicken meat fillets. The antimicrobial agents were added individually or in combination. As a result, nisin + CEO, nisin + REO, CEO + REO samples had the lowest final *L. monocytogenes* counts (6.3–6.6 log CFU/g) as compared to nisin, CEO, REO and control samples (8–8.6 log CFU/g). Significant higher bacterial reductions indicated that when used in combination, the antimicrobials had stronger effect in controlling the *L. monocytogenes* population on chicken samples than using in separate. Xu et al. (2007) indicated that nisin alone did not induce a significant reduction in *Salmonella* and *L. monocytogenes*, but when tested in combination with GSE or citric acid, significant reductions (2.5–2.8 log CFU/g) of were observed.

3.1.2. Antimicrobial kinetics of *L. monocytogenes* inoculated on shrimps

Four inactivation (linear, Weibull, Huang's, and Fermi) models were used to evaluate the antimicrobial effect of each treatment. The fitting curves are presented in Fig. 2 while the goodness-of-fit (as represented by RMSE, SSE, AIC and BIC values) are shown in Table 1. In nisin and GSE treated groups, Weibull model provided good statistical fitness with the lowest RMSE (0.16 and 0.14, respectively) as compared to Fermi, linear and Huang's models. Similarly, lower RMSE (0.06–0.14) values in combination group were recorded by Weibull model ($P < 0.05$). Moreover, AIC and BIC are also regarded as important parameters indicating the overfitting status. The lower the values, the better the fittings are (Nyhan et al., 2018). Smaller values of SSE (0.03–0.13), AIC (ranging from −31.46 to −16.42), as well as BIC (ranging from −34.07 to −19.04) for Weibull models were observed in all treatments, regardless of strain type. These results indicated that the Weibull model was statistically suitable in describing the relationship between the treatment time of each antimicrobial agent and the survival of *L. monocytogenes* on shrimps. In a previous study, the Weibull

Table 1
Fitting goodness of inactivation models describing the *L. monocytogenes* reduction.

Strain	Treatment	Model	RMSE	SSE	AIC	BIC
SSA184	Nisin	Linear	0.18 ± 0.01 ^{op}	0.10 ± 0.02 ^{fghi}	−19.16 ± 1.66 ^{efgh}	−21.78 ± 1.66 ^{efgh}
		Weibull	0.09 ± 0.01 ^{abcd}	0.06 ± 0.01 ^{abcd}	−24.23 ± 1.38 ^{bc}	−26.84 ± 1.38 ^{bc}
		Huang's	0.23 ± 0.02 ^{q}	0.14 ± 0.02 ^{jklm}	−15.73 ± 1.18 ^{ijkl}	−18.34 ± 1.18 ^{ijkl}
		Fermi	0.17 ± 0.02 ^{nop}	0.08 ± 0.01 ^{bcdefg}	−21.31 ± 1.03 ^{de}	−23.92 ± 1.03 ^{de}
	GSE	Linear	0.17 ± 0.01 ^{nop}	0.20 ± 0.03 ^{pq}	−11.98 ± 1.00 ^{no}	−14.59 ± 0.99 ^{no}
		Weibull	0.14 ± 0.02 ^{ijklmn}	0.09 ± 0.01 ^{defgh}	−20.12 ± 0.91 ^{defg}	−22.73 ± 0.91 ^{defg}
		Huang's	0.15 ± 0.01 ^{jklmn}	0.15 ± 0.02 ^{klmn}	−15.03 ± 1.10 ^{jklm}	−17.64 ± 1.13 ^{jklm}
		Fermi	0.16 ± 0.01 ^{lmnop}	0.11 ± 0.01 ^{ghij}	−18.10 ± 0.74 ^{fghi}	−20.71 ± 0.74 ^{fghi}
	Combination	Linear	0.16 ± 0.02 ^{lmnop}	0.15 ± 0.02 ^{klmn}	−14.93 ± 1.02 ^{jklm}	−17.64 ± 1.10 ^{jklm}
		Weibull	0.09 ± 0.01 ^{bcde}	0.10 ± 0.01 ^{fghi}	−19.06 ± 0.82 ^{efgh}	−21.67 ± 0.82 ^{efgh}
		Huang's	0.13 ± 0.01 ^{ghijkl}	0.16 ± 0.01 ^{lmn}	−14.57 ± 0.81 ^{jklmn}	−17.18 ± 0.81 ^{jklmn}
		Fermi	0.10 ± 0.01 ^{cdefg}	0.12 ± 0.01 ^{hijk}	−17.23 ± 0.68 ^{ghij}	−19.84 ± 0.68 ^{ghij}
SSA97	Nisin	Linear	0.13 ± 0.02 ^{fghijk}	0.09 ± 0.02 ^{efgh}	−19.91 ± 1.91 ^{defg}	−22.52 ± 1.90 ^{defg}
		Weibull	0.08 ± 0.01 ^{abcd}	0.05 ± 0.01 ^{ab}	−26.09 ± 1.66 ^{b}	−28.71 ± 1.59 ^{b}
		Huang's	0.11 ± 0.01 ^{defgh}	0.07 ± 0.01 ^{bcdef}	−22.66 ± 1.18 ^{cd}	−25.28 ± 1.17 ^{cd}
		Fermi	0.07 ± 0.02 ^{abc}	0.06 ± 0.01 ^{abcd}	−24.23 ± 1.38 ^{bc}	−26.84 ± 1.38 ^{bc}
	GSE	Linear	0.15 ± 0.01 ^{jklmn}	0.18 ± 0.02 ^{nop}	−13.40 ± 1.19 ^{klmno}	−16.02 ± 1.20 ^{klmno}
		Weibull	0.07 ± 0.02 ^{ab}	0.13 ± 0.01 ^{ijkl}	−16.42 ± 0.63 ^{hijk}	−19.04 ± 0.62 ^{hijk}
		Huang's	0.13 ± 0.02 ^{hijklm}	0.17 ± 0.01 ^{mno}	−13.73 ± 0.48 ^{klmn}	−16.34 ± 0.48 ^{klmn}
		Fermi	0.12 ± 0.01 ^{fghijk}	0.14 ± 0.01 ^{jklm}	−15.68 ± 0.58 ^{ijkl}	−18.29 ± 0.56 ^{ijkl}
	Combination	Linear	0.19 ± 0.01 ^{p}	0.17 ± 0.02 ^{mno}	−13.77 ± 0.97 ^{klmn}	−16.38 ± 0.98 ^{klmn}
		Weibull	0.08 ± 0.01 ^{abcd}	0.08 ± 0.01 ^{cdefg}	−20.92 ± 1.18 ^{def}	−23.53 ± 1.17 ^{def}
		Huang's	0.10 ± 0.01 ^{cdefg}	0.16 ± 0.01 ^{lmn}	−14.57 ± 0.81 ^{jklmn}	−17.18 ± 0.79 ^{jklmn}
		Fermi	0.10 ± 0.01 ^{cdefg}	0.09 ± 0.02 ^{efgh}	−19.90 ± 1.95 ^{defg}	−22.51 ± 1.94 ^{defg}
LM10	Nisin	Linear	0.15 ± 0.02 ^{jklmn}	0.15 ± 0.02 ^{klmn}	−15.11 ± 1.66 ^{jklm}	−17.72 ± 1.66 ^{jklm}
		Weibull	0.12 ± 0.01 ^{efghij}	0.11 ± 0.01^{ghij}	−18.10 ± 0.74 ^{fghi}	−20.71 ± 0.74 ^{fghi}
		Huang's	0.14 ± 0.01 ^{ijklmn}	0.17 ± 0.02 ^{mno}	−13.77 ± 0.97 ^{klmn}	−16.38 ± 0.97 ^{klmn}
		Fermi	0.11 ± 0.01 ^{defghi}	0.13 ± 0.01 ^{ijkl}	−16.42 ± 0.63 ^{hijk}	−19.04 ± 0.63 ^{hijk}
	GSE	Linear	0.12 ± 0.01 ^{efghij}	0.09 ± 0.01 ^{defgh}	−20.12 ± 0.91 ^{defg}	−22.73 ± 0.91 ^{defg}
		Weibull	0.06 ± 0.01 ^{a}	0.03 ± 0.01 ^{a}	−31.46 ± 2.84 ^{a}	−34.07 ± 2.84 ^{a}
		Huang's	0.08 ± 0.01 ^{abcd}	0.06 ± 0.02 ^{bcde}	−24.00 ± 2.77 ^{bc}	−26.61 ± 2.77 ^{bc}
		Fermi	0.08 ± 0.02 ^{abcd}	0.05 ± 0.00 ^{abc}	−25.35 ± 0.86 ^{bc}	−27.96 ± 0.86 ^{bc}
	Combination	Linear	0.15 ± 0.01 ^{klmno}	0.19 ± 0.02 ^{op}	−12.49 ± 1.06 ^{mno}	−15.10 ± 1.06 ^{mno}
		Weibull	0.12 ± 0.01 ^{efghij}	0.12 ± 0.01 ^{hijk}	−17.23 ± 0.68 ^{ghij}	−19.84 ± 0.68 ^{ghij}
		Huang's	0.16 ± 0.02 ^{mnop}	0.18 ± 0.02 ^{nop}	−13.22 ± 1.25 ^{lmno}	−15.84 ± 1.25 ^{lmno}
		Fermi	0.15 ± 0.01 ^{jklmno}	0.23 ± 0.02 ^{q}	−10.74 ± 0.97°	−13.36 ± 0.97°

*Notes: Root Mean Squared Error (RMSE), Sum of Squares for Error (SSE), Akaike Information Criterion (AIC) and Bayesian Information Criterion (BIC). Within the same column, values with different lowercase letters are significantly different ($P < 0.05$).

model with the lowest RMSE and AIC was verified as the most superior model to describe antimicrobial effects of lactic acid and sodium hypochlorite against *L. innocua* on fresh produce (Chen et al., 2019).

To further understand the antimicrobial effect of nisin and GSE on *L. monocytogenes* inoculated on shrimps, the estimated fitting parameters of inactivation models were determined (Table S1). The analysis of these kinetic parameters can provide us valuable information about sensitivity and resistance of *L. monocytogenes* against different treatments during inactivation process. For linear model, combined nisin and GSE presented highest general inactivation rate (0.12–0.14 log CFU/g/min), followed by nisin (0.07–0.10 log CFU/g/min) and GSE (0.04–0.07 log CFU/g/min) treatments. For Weibull fitting, the time needed to achieve 1 log CFU/g reduction of *L. monocytogenes* SSA184, SSA97 and LM10 by combined treatment were 6.90, 9.01 and 8.20 min, respectively. Based on the results of Huang's fitting, the combination treatment resulted in the significantly greater maximum antibacterial rate (0.12–0.14 log CFU/g/min) as compared to the respective nisin- or GSE-treated samples ($P < 0.5$). Under the same treatment, the SSA97 and LM10 strains showed longer lag phases as compared to *L. monocytogenes* SSA184, suggesting that they were more tolerate to nisin and GSE stresses. These findings were supported by Bertrand (2019) who indicated that bacteria with longer lag phase are more tolerant to external stresses such as antibiotics. Furthermore, the combination and nisin groups showed the significantly faster specific decay rate as compared to the GSE treatment ($P < 0.05$). These findings collectively verified that the combination treatment presented an enhanced antimicrobial effect against all tested strains and SSA184 showed the highest susceptibility to nisin and GSE treatments.

3.2. Residual effects of nisin and GSE against L. monocytogenes

3.2.1. Growth dynamics of L. monocytogenes on shrimps during refrigeration

Sublethally injured *L. monocytogenes* cells might be induced by nisin

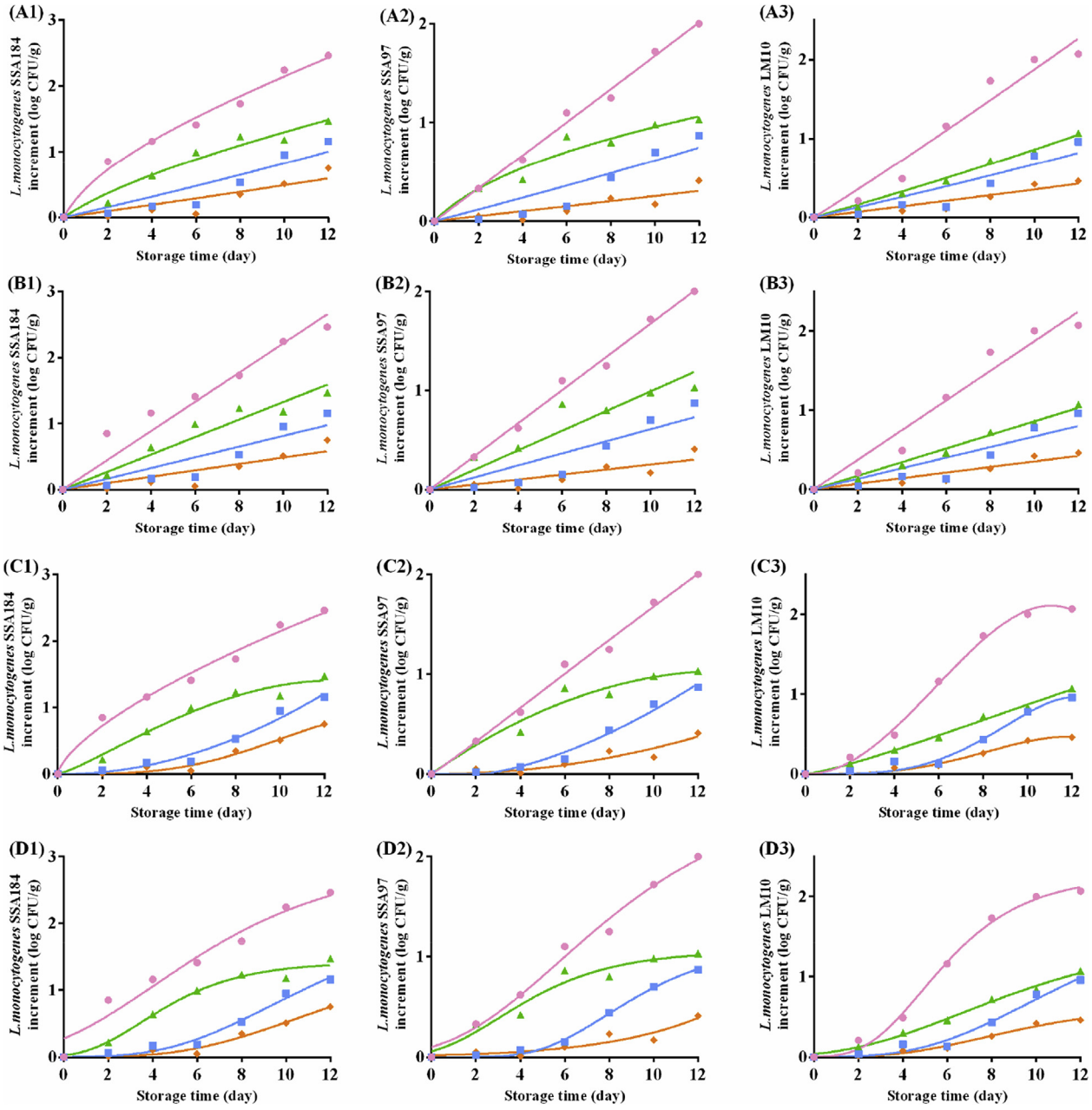

Fig. 3. Growth modelling of *L. monocytogenes* during refrigerated storage. (A) Modified Gompertz, (B) Exponential, (C) Beta function and (D) Baranyi models.

and GSE treatments and these sublethally cells should be taken into consideration as they can recover and regain pathogenicity under suitable conditions. Therefore, the survival of normal and sublethally injured *L. monocytogenes* SSA184, SSA97 and LM10 on shrimps during 12-day refrigeration were evaluated (Fig. 1B). Increasing tendencies were observed in all control samples during storage at 4 °C. The populations of *L. monocytogenes* SSA184, SSA97 and LM10 progressively increased during 12-day storage by 2.5, 1.7 and 2.0 log CFU/g, respectively. The nisin and GSE treated shrimps had significantly lower *L. monocytogenes* recovery as compared with the control group ($P < 0.05$). Similar findings were reported for the inhibited *L. monocytogenes* growth (4 °C) on chicken meat treated with nisin and on minced trout fillet treated with GSE (Kakaei & Shahbazi, 2016; Raeisi et al., 2016). During storage, the residual antilisterial efficacy of GSE was comparable with that of nisin. It is postulated that the decrease of membrane fluidity was responsible for the decreased antilisterial effect of nisin at low storage temperatures (Solomakos et al., 2008).

In addition, it is interesting to note that the residual effect of nisin during storage was time-dependent. At the early stage of storage, the populations of nisin-treated cells were similar (SSA97 and LM10) or slightly increased (SSA184) as compared to the respective initial counts (day 0). However, nisin showed a weaker antilisterial effect of nisin at the later period of storage (from day 6 to day 12), regardless of the strain type, indicating that the antimicrobial efficacy of nisin was highly depending on the properties of the food in contact with. A previous report indicated the capability of glutathione in inactivating nisin (Gharsallaoui, Oulahal, Joly, & Degraeve, 2016). The loss of nisin activity is related to the formation of nisin-glutathione adduct mediated by glutathione transferase (Stergiou, Thomas, & Adams, 2006). Nisin can also react with the fat such as phospholipids (Deegan, Cotter, Hill, & Ross, 2006). Oshima et al. (2014) investigated the residual nisin which was added to milk pudding (containing 5% or 7.5% milk fat). As a result, 25–50% nisin activity was lost after 15-day storage. Considering that glutathione, glutathione-transferase, lipid, etc., are commonly existed in shrimp flesh, the antilisterial effect of nisin was partially and gradually compromised along with the storage due to its interaction with these components. Moreover, the sustainability of nisin was largely associated with the pH value. It is well-known that nisin is

Table 2
Fitting goodness of models describing the growth of *L. monocytogenes* during storage.

Strain	Treatment	Model	RMSE	SSE	AIC	BIC
SSA184	Control	Gompertz	0.32 ± 0.02 ^{s}	0.35 ± 0.01 ^{p}	0.58 ± 0.19 ^{w}	0.37 ± 0.19 ^{w}
		Exponential	0.25 ± 0.04 ^{r}	0.36 ± 0.03 ^{p}	−5.24 ± 0.57 ^{stu}	−5.29 ± 0.57 ^{stu}
		Beta function	0.26 ± 0.01 ^{r}	0.28 ± 0.03 *	−2.86 ± 0.71 ^{v}	−3.03 ± 0.71 ^{v}
		Baranyi	0.20 ± 0.02 ^{opq}	0.19 ± 0.03 ^{mn}	−7.58 ± 1.04 ^{nopqr}	−7.69 ± 1.04 ^{nopqr}
	Nisin	Gompertz	0.17 ± 0.03 ^{lmnop}	0.19 ± 0.01 ^{mn}	−3.52 ± 0.45 ^{uv}	−3.73 ± 0.45 ^{uv}
		Exponential	0.15 ± 0.02 ^{ghijklm}	0.13 ± 0.02 ^{jkl}	−12.34 ± 0.89 ^{fgh}	−12.39 ± 0.89 ^{fgh}
		Beta function	0.15 ± 0.02 ^{ghijklm}	0.10 ± 0.02 ^{efghij}	−10.21 ± 1.16 ^{hijklm}	−10.38 ± 1.16 ^{hijklm}
		Baranyi	0.12 ± 0.01 ^{cdefg}	0.06 ± 0.01 ^{bcde}	−15.45 ± 1.35 ^{cd}	−15.56 ± 1.35 ^{cd}
	GSE	Gompertz	0.25 ± 0.03 ^{r}	0.19 ± 0.02 ^{mn}	−3.65 ± 0.60 ^{uv}	−3.87 ± 0.60 ^{uv}
		Exponential	0.27 ± 0.02 ^{r}	0.43 ± 0.04 ^{q}	−3.88 ± 0.59 ^{tuv}	−3.93 ± 0.59 ^{tuv}
		Beta function	0.19 ± 0.03 ^{mnopq}	0.14 ± 0.01 ^{kl}	−7.77 ± 0.41 ^{nopqr}	−7.94 ± 0.41 ^{nopqr}
		Baranyi	0.13 ± 0.01 ^{efghijk}	0.08 ± 0.01 ^{defg}	−13.72 ± 0.72 ^{def}	−13.83 ± 0.72 ^{def}
	Combination	Gompertz	0.16 ± 0.04 ^{ijklmno}	0.14 ± 0.01 ^{kl}	−5.77 ± 0.41 ^{rst}	−5.99 ± 0.41 ^{rst}
		Exponential	0.18 ± 0.05 ^{mnopq}	0.18 ± 0.02 ^{m}	−10.03 ± 0.64 ^{c}	−10.09 ± 0.64 ^{c}
		Beta function	0.11 ± 0.03 ^{bcdef}	0.13 ± 0.01 ^{jkl}	−8.30 ± 0.48 ^{mnopq}	−8.46 ± 0.48 ^{mnopq}
		Baranyi	0.11 ± 0.04 ^{bcdef}	0.10 ± 0.01 ^{efghij}	−12.14 ± 0.57 ^{fghi}	−12.25 ± 0.57 ^{fghi}
SSA97	Control	Gompertz	0.16 ± 0.01 ^{hijklmn}	0.08 ± 0.01 ^{defg}	−9.72 ± 0.72 ^{jklmn}	−9.93 ± 0.72 ^{jklmn}
		Exponential	0.16 ± 0.02 ^{hijklmno}	0.14 ± 0.01 ^{l}	−11.61 ± 0.47 ^{fghij}	−11.67 ± 0.47 ^{fghij}
		Beta function	0.12 ± 0.01 ^{efghij}	0.10 ± 0.01 ^{fghijk}	−9.94 ± 0.83 ^{ijklm}	−11.88 ± 0.83 ^{ijklm}
		Baranyi	0.12 ± 0.01 ^{efghij}	0.06 ± 0.01 ^{abcd}	−15.76 ± 0.96 ^{bc}	−10.10 ± 0.96 ^{bc}
	Nisin	Gompertz	0.13 ± 0.01 ^{efghijk}	0.14 ± 0.01 ^{kl}	−5.77 ± 0.41 ^{rst}	−5.99 ± 0.41 ^{rst}
		Exponential	0.29 ± 0.03 ^{bcde}	0.50 ± 0.04 ^{r}	−2.92 ± 0.53 ^{v}	−2.92 ± 0.53 ^{v}
		Beta function	0.09 ± 0.02 ^{abcd}	0.08 ± 0.01 ^{defgh}	−11.47 ± 1.03 ^{fghijk}	−11.63 ± 1.03 ^{fghijk}
		Baranyi	0.08 ± 0.00 ^{abc}	0.03 ± 0.00 ^{a}	−21.49 ± 1.34 ^{a}	−21.60 ± 1.34 ^{a}
	GSE	Gompertz	0.17 ± 0.02 ^{klmno}	0.12 ± 0.01 ^{hijk}	−6.86 ± 0.48 ^{pqrs}	−7.07 ± 0.48 ^{pqrs}
		Exponential	0.12 ± 0.00 ^{efghij}	0.12 ± 0.00 ^{ghijkl}	−13.04 ± 0.29 ^{efg}	−13.10 ± 0.29 ^{efg}
		Beta function	0.14 ± 0.02 ^{fghijkl}	0.09 ± 0.01 ^{defghi}	−10.88 ± 0.64 ^{ghijkl}	−11.05 ± 0.64 ^{ghijkl}
		Baranyi	0.10 ± 0.01 ^{bcdef}	0.07 ± 0.01 ^{bcdef}	−15.02 ± 0.95 ^{cde}	−15.13 ± 0.95 ^{cde}
	Combination	Gompertz	0.11 ± 0.01 ^{cdefg}	0.06 ± 0.01 ^{abcd}	−11.76 ± 0.96 ^{fghij}	−11.98 ± 0.96 ^{fghij}
		Exponential	0.08 ± 0.01 ^{abcd}	0.07 ± 0.01 ^{bcdef}	−17.02 ± 0.95 ^{c}	−17.08 ± 0.95 ^{c}
		Beta function	0.10 ± 0.02 ^{cdef}	0.06 ± 0.01 ^{bcde}	−13.33 ± 0.51 ^{ef}	−13.50 ± 0.51 ^{ef}
		Baranyi	0.06 ± 0.01 ^{ab}	0.03 ± 0.01 ^{ab}	−20.30 ± 2.62 ^{ab}	−20.41 ± 2.62 ^{ab}
LM10	Control	Gompertz	0.21 ± 0.03 ^{pq}	0.20 ± 0.02 ^{mn}	−3.18 ± 0.63 ^{uv}	−3.40 ± 0.63 ^{uv}
		Exponential	0.19 ± 0.01 ^{nopq}	0.22 ± 0.02 ^{n}	−8.75 ± 0.74 ^{lmnop}	−8.80 ± 0.74 ^{lmnop}
		Beta function	0.19 ± 0.00 ^{mnopq}	0.07 ± 0.00 ^{cdef}	−12.30 ± 0.44 ^{fgh}	−12.47 ± 0.44 ^{fgh}
		Baranyi	0.05 ± 0.02 ^{a}	0.03 ± 0.01 ^{ab}	−20.30 ± 2.62 ^{ab}	−20.41 ± 2.62 ^{ab}
	Nisin	Gompertz	0.15 ± 0.01 ^{ghijklm}	0.12 ± 0.02 ^{ijkl}	−6.72 ± 1.01 ^{pqrs}	−6.94 ± 1.01 ^{pqrs}
		Exponential	0.22 ± 0.03 ^{q}	0.30 ± 0.03*	−6.53 ± 0.64 ^{qrs}	−6.59 ± 0.64 ^{qrs}
		Beta function	0.15 ± 0.02 ^{ghijklm}	0.08 ± 0.02 ^{defg}	−11.83 ± 1.46 ^{fghij}	−11.99 ± 1.46 ^{fghij}
		Baranyi	0.11 ± 0.01 ^{cdefg}	0.05 ± 0.01 ^{abcd}	−16.71 ± 1.61 ^{c}	−16.81 ± 1.61 ^{c}
	GSE	Gompertz	0.17 ± 0.03 ^{lmnop}	0.08 ± 0.00 ^{defgh}	−9.41 ± 0.39 ^{klmno}	−9.62 ± 0.39 ^{klmno}
		Exponential	0.13 ± 0.02 ^{efghijk}	0.08 ± 0.01 ^{defgh}	−16.66 ± 0.83 ^{cd}	−16.72 ± 0.83 ^{cd}
		Beta function	0.12 ± 0.02 ^{efghij}	0.07 ± 0.01 ^{bcdef}	−12.66 ± 0.82 ^{fg}	−12.83 ± 0.82 ^{fg}
		Baranyi	0.10 ± 0.01 ^{bcdef}	0.04 ± 0.00 ^{abc}	−19.20 ± 0.95 ^{b}	−19.31 ± 0.95 ^{b}
	Combination	Gompertz	0.09 ± 0.01 ^{bcde}	0.11 ± 0.02 ^{ghijkl}	−7.33 ± 1.11 ^{opqrs}	−7.54 ± 1.11 ^{opqrs}
		Exponential	0.13 ± 0.02 ^{efghijk}	0.12 ± 0.02 ^{hijkl}	−12.91 ± 0.96 ^{fg}	−12.96 ± 0.96 ^{fg}
		Beta function	0.11 ± 0.01 ^{cdef}	0.08 ± 0.01 ^{defg}	−11.72 ± 0.72 ^{fghij}	−11.88 ± 0.72 ^{fghij}
		Baranyi	0.06 ± 0.02 ^{ab}	0.06 ± 0.00 ^{abcd}	−15.69 ± 0.60 ^{c}	−16.23 ± 0.60 ^{c}

*Notes: Sum of Squares for Error (SSE), Root Mean Squared Error (RMSE), Akaike Information Criterion (AIC) and Bayesian Information Criterion (BIC). Within the same column, values with different lowercase letters are significantly different ($P < 0.05$).

very active at acidic condition but losses its activity dramatically at basic condition (Müller-Auffermann, Grijalva, Jacob, & Hutzler, 2015). The initial pH of shrimp was around 6.5 but it increased to 7.9 after 12-day storage (Okpala, 2015). Such change of pH in shrimp during storage could reduce the activity of nisin in inhibiting the *L. monocytogenes* growth.

The binary application of nisin and GSE was found to be more effective in suppressing the growth of all *L. monocytogenes* strains during shrimp storage than using in separate. Specifically, the populations of SSA184, SSA97 and LM10 on tilapia samples stored at 4 °C were increased by 1.0, 1.0 and 1.2 log CFU/g, respectively. It might be due to the interaction between nisin and GSE by ion cross-linking which can improve the stability of nisin and maintain the antimicrobial effect during prolonged refrigerated storage (Gong et al., 2018; Wu, Yu, & Flint, 2017).

3.2.2. Growth modelling of *L. monocytogenes* on shrimps during storage

Four growth models were used for fitting *L. monocytogenes* count increment during prolonged storage (4 °C). The fitting curves and fitting goodness are shown in Fig. 3 and Table 2, respectively. Generally, the Beta function and Baranyi models exhibited excellent fitting for all four groups, regardless of strain type. Nevertheless, further analysis indicate that the Baranyi equation was the most superior one in describing the isothermal (4 °C) growth of *L. monocytogenes* as the lowest RMSE (0.05–0.20), SSE (0.03–0.19), AIC (ranging from −21.49 to −7.58) and BIC (ranging from −21.60 to −7.69) values were obtained by this model. Therefore, we conclude that the Baranyi model in describing the effect of nisin and GSE on the growth kinetics of *L. monocytogenes* on shrimps during cold storage. The results are consistent with a previous report which evaluated four predictive models for the growth of *L. monocytogenes* in vacuum-packaged chilled pork (Ye et al., 2013). Based on the goodness-of-fit results, Baranyi model (MSE: 0.03–0.06; $1.00 \leq B_f \leq A_f \leq 1.06$) was sufficient to describe the growth curves of *L. monocytogenes* in pork samples stored under various conditions (4, 10, 15, 20 and 25 °C).

The determination of the model parameters further provided useful information about the growing status of each strain and their sensitivity to nisin and GSE during refrigeration (Table S2). For instance, the microbial growth rate was strain-dependent; however, the general growth rates (0.06–0.11 log CFU/g/day) of a certain strain were always lower in the combination group as compared with other treatment groups ($P < 0.05$). On the other hand, the absence of x_m for some growth curves (control SSA184 and GSE-treated SSA97) suggests that the maximum growing rate is reached at the initial of the storage (Ochoa-Velasco et al., 2018). Higher listerial loads (Q) were always observed in control groups than in nisin and/or GSE treated cells during storage; this might be an indication of residual antimicrobial effects of nisin and GSE against three tested *L. monocytogenes* strains. Moreover, the time required to reach the largest listerial growth (x_Q) was significantly affected by the nisin and GSE treatments. As suggested by the Baranyi model, the combination treatment resulted in the lowest maximum bacterial growth of *L. monocytogenes* SSA184 (0.91 log CFU/g), SSA97 (0.88 log CFU/g) and LM10 (1.02 log CFU/g) cells during storage. It is also notable to highlight the lag phase period, which suggests the time when the bacterium is adapting itself to the growth situation and is not able to divide, became significantly lengthened after combined treatment ($P < 0.05$) (Valdivia-Nájar, Martín-Belloso, Giner-Seguí, & Soliva-Fortuny, 2017). Specifically, the λ values for the control SSA184, SSA97 and LM10 were 26.80, 34.14 and 20.59 days, respectively. At the same time, for combination groups, the λ values increased to 40.87–68.45 days. Overall, these findings indicated superior antimicrobial effect of the combined treatment on inhibiting the growth of three *L. monocytogenes* strains at low temperature.

3.3. Model verification

According to the results of model fitting analysis, the Weibull model is the best inactivation model in describing the inactivation kinetics of nisin and GSE while the Baranyi model best predicted the growth dynamics of *L. monocytogenes* during storage.

To validate the performance of selected models, additional data (inactivation process: 7.5 min; storage: day 7) were used for the comparison of predicted and observed values. Several performance indices were calculated and shown in Table 3. The B_f describe the consistency between experimental value and predicted data, and thus provide an overall objective indication of model performance. A_f value afford additional indication as it provides an average accuracy of prediction by calling off under or over estimations. The closer the value gets to 1, the better the model is (Ye et al., 2013). For the Weibull model, it is observed that all the A_f and B_f values were in the range of $1.00 \leq B_f \leq A_f \leq 1.10$ while the D% and B% values were within the scope of $-1 \leq B\% \leq D\% \leq 10$. These results further confirmed the goodness of Weibull model in predicting the inactivation effects of nisin and GSE, which is in accordance with a previous study (Ghate et al., 2017).

Similarly, the performance of Baranyi model as growth model was also analysed. It is suggested that the for the growth models, a B_f value ranging from 0.9 to 1.05 is regarded as quite good. If B_f value determined in the rage of 1.05–1.15 or 0.7–0.9, then the model is acceptable to describe bacterial growth rate. However, a model whose B_f value is smaller than 0.7 or larger than 1.15 is inapplicable (Nyhan et al., 2018). The goodness of Baranyi model in describing the growth of inoculated *L. monocytogenes* has been verified in previous studies (Omac, Moreira, & Castell-Perez, 2018; Rodríguez, Alcalá, Gimeno, & Cosano, 2000). In this study, all calculated B_f values for Baranyi model

Table 3
Performance indices of Weibull and Baranyi models.

Strain	Treatment	Weibull model (7.5 min)						Baranyi model (day 7)					
		u_p	u_o	A_f	B_f	D%	B%	u_p	u_o	A_f	B_f	D%	B%
SSA184	Control	–	–	–	–	–	–	7.67 ± 0.08	7.61 ± 0.12	1.04	1.01	4	1
	Nisin	5.61 ± 0.01	5.32 ± 0.01	1.10	1.05	10	5	5.31 ± 0.04	5.02 ± 0.12	1.11	1.06	11	6
	GSE	6.01 ± 0.00	5.76 ± 0.17	1.09	1.04	9	4	6.16 ± 0.05	6.31 ± 0.20	1.06	0.98	6	−2
	Combination	5.19 ± 0.02	5.07 ± 0.11	1.06	1.03	6	3	4.66 ± 0.02	4.51 ± 0.06	1.06	1.03	6	3
SSA97	Control	–	–	–	–	–	–	6.99 ± 0.11	6.96 ± 0.13	1.06	1.00	6	0
	Nisin	5.39 ± 0.01	5.20 ± 0.12	1.08	1.04	8	4	5.30 ± 0.02	5.19 ± 0.04	1.04	1.02	4	2
	GSE	5.59 ± 0.01	5.62 ± 0.03	1.01	1.00	1	0	6.02 ± 0.02	6.08 ± 0.09	1.03	0.99	3	−1
	Combination	5.07 ± 0.02	5.02 ± 0.18	1.06	1.01	6	1	4.40 ± 0.02	4.40 ± 0.06	1.03	1.00	3	0
LM10	Control	–	–	–	–	–	–	7.52 ± 0.06	7.69 ± 0.10	1.05	0.98	5	−2
	Nisin	5.63 ± 0.01	5.65 ± 0.05	1.02	1.00	2	0	5.58 ± 0.05	5.41 ± 0.07	1.06	1.03	6	3
	GSE	5.85 ± 0.00	5.83 ± 0.08	1.03	1.01	3	1	6.17 ± 0.09	6.18 ± 0.12	1.03	1.00	3	0
	Combination	5.28 ± 0.01	5.26 ± 0.11	1.03	1.00	3	0	4.72 ± 0.02	4.68 ± 0.05	1.02	1.01	2	1

*Notes: u_p: predicted value; u_o: observed value; A_f: Accuracy factor; B_f: Bias factor; D%: discrepancy percentage; B%: bias percentage.

(0.98–1.06) indicated that the model was good for predicting the growth kinetics of *L. monocytogenes* during cold storage. Moreover, determined A_f (1.02–1.11) and D% (2%–6%) values further suggest that the predicted data were quite close to experimental data. Thus, the Baranyi model is applicable in describe the growth kinetics of *L. monocytogenes* on shrimps during refrigerated storage.

3.4. Morphological changes of *L. monocytogenes*

To preliminarily evaluate the antilisterial mechanism of nisin and GSE, AFM analysis was conducted to reveal the morphological changes of *L. monocytogenes* cells (Liu & Yang, 2019). According to the captured images (Fig. 4A–C), all three *L. monocytogenes* strains in the control

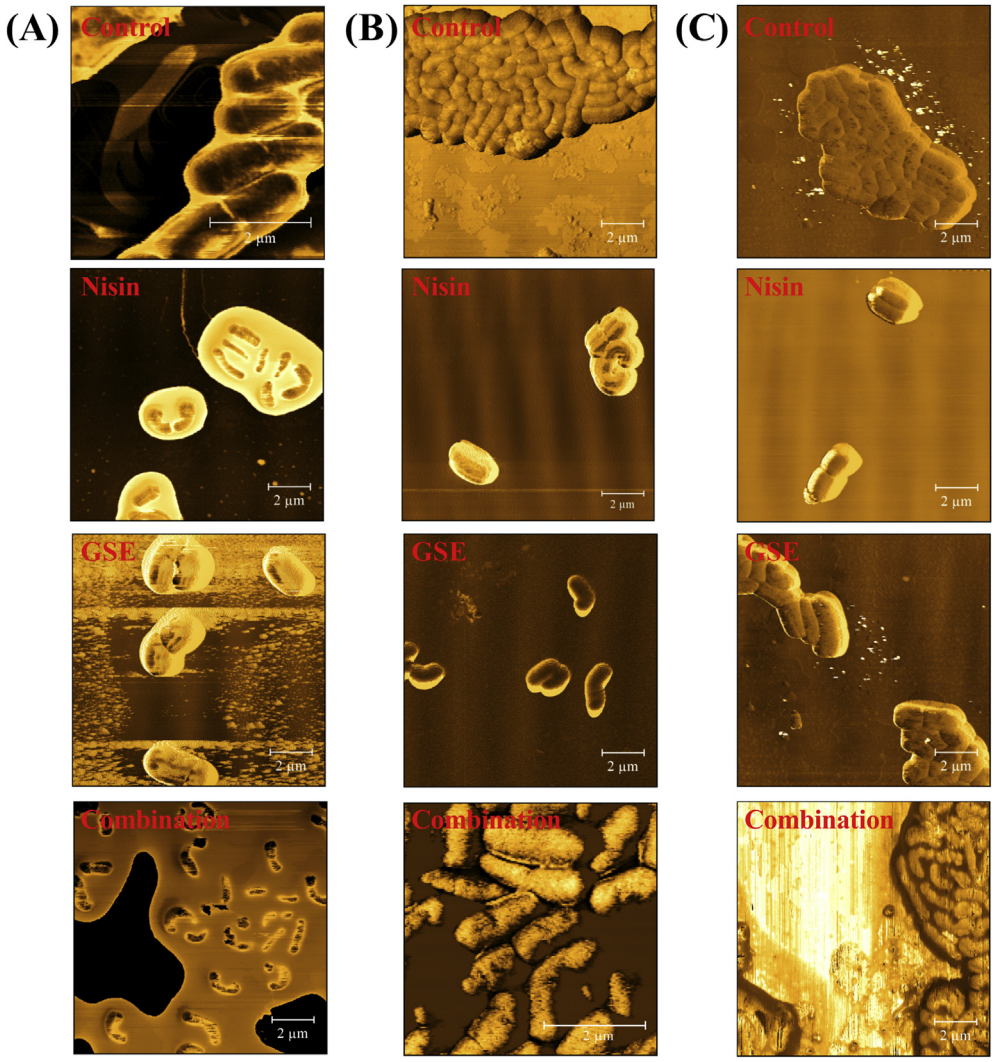

(D)

Strain	Treatment	Width (μm)	Height (μm)	RMS roughness (nm)
SSA184	Control	0.78 ± 0.05 ^{cdef}	0.41 ± 0.04 ^{cde}	3.57 ± 0.59 ^{a}
	Nisin	0.59 ± 0.08 ^{ab}	0.30 ± 0.03 ^{ab}	7.77 ± 0.78 ^{c}
	GSE	0.63 ± 0.04 ^{bc}	0.35 ± 0.07 ^{bcd}	5.22 ± 1.19 ^{ab}
	Combination	0.47 ± 0.10 ^{a}	0.25 ± 0.02 ^{a}	10.12 ± 0.54 ^{d}
SSA97	Control	0.90 ± 0.09 ^{efg}	0.45 ± 0.04 ^{de}	3.93 ± 0.56 ^{ab}
	Nisin	0.79 ± 0.04 ^{cdef}	0.41 ± 0.03 ^{cde}	8.92 ± 0.77 ^{cd}
	GSE	0.86 ± 0.02 ^{def}	0.47 ± 0.07 ^{e}	5.06 ± 0.43 ^{ab}
	Combination	0.73 ± 0.07 ^{bcd}	0.39 ± 0.02 ^{bcde}	9.27 ± 0.92 ^{cd}
LM10	Control	1.03 ± 0.10 ^{g}	0.47 ± 0.06 ^{e}	4.49 ± 0.45 ^{ab}
	Nisin	0.83 ± 0.06 ^{def}	0.33 ± 0.07 ^{abc}	9.01 ± 0.65 ^{cd}
	GSE	0.94 ± 0.09 ^{fg}	0.41 ± 0.06 ^{cde}	5.66 ± 0.60 ^{b}
	Combination	0.77 ± 0.04 ^{cde}	0.31 ± 0.02 ^{abc}	9.19 ± 1.52 ^{cd}

Fig. 4. Atomic force microscopy (AFM) images of *L. monocytogenes* SSA184 (A), SSA97 (B) and LM10 (C) under different treatments; (D) Changes in width, length and root mean squared (RMS) roughness. Note: within the same column, values with different lowercase letters are significantly different ($P < 0.05$).

group showed intact, plump and smooth surface. Generally, the morphology of GSE-treated bacterial cells presented similar rod shape to that of untreated cells. However, some bulge and wrinkles were observed on the cell surface. As for the samples treated with nisin or its combination with GSE, cell structures became deformed as compared with natural shape and cell surface turned coarse, irregular with some pores on it, indicating the partial destroy of bacterial cells. Moreover, the bacterial cells aggregated together without distinct cellular boundaries. These findings were in accordance with a previous research, showing that cell surface became rough and cell walls were severely damaged after exposure to nisin (Liu, Pei, Han, Feng, & Li, 2015).

Furthermore, the bacterial cells treated with combined nisin and GSE were markedly distorted or even ruptured as some fragments were observed. It is notable that after exposure to nisin or its combination with GSE, the cells presented some wrinkles and residues in the surface of cell membranes which might be the exudative intracellular substances such as protein, nucleic acid and the destroyed lipid bilayer structure (Jin, Zhang, & Boyd, 2010). A previous study indicated that combined nisin and GSE showed enhanced antimicrobial effect against *L. monocytogenes* by forming pores, inducing leakage of cytoplasmic biomacromolecules as well as disturbing pivotal intracellular metabolism (Zhao et al., 2020).

Quantitative analysis completed using Gwyddion software further uncovered the dimensional changes of the *L. monocytogenes* (Fig. 4D). The width of *L. monocytogenes* SSA184, SSA97 and LM10 cells imaged by AFM were 0.78, 0.90, and 1.03 μm, respectively. No significant difference in width (0.63–0.94 μm) was observed between the GSE-treated cells and the respective control samples ($P > 0.05$). However, the width of all tested *L. monocytogenes* strains decreased after antimicrobial treatments of nisin and its combination with GSE by up to 24.36% and 39.74%, respectively.

Similar findings were observed for the changes in height. The heights of individual control cells were 0.41, 0.45 and 0.47 μm for SSA184, SSA97 and LM10, respectively. Nisin and its combination with GSE significantly reduced the cell width, especially for the SSA184 strain ($P < 0.05$). Specifically speaking, the combined treatment reduced the cell width of SSA184 to 0.25 μm, followed by the nisin treatment (0.30 μm). Furthermore, RMS roughness was further measured to evaluate surface morphological variations. The RMS roughness values of each control group were kept as a relatively low level (3.57–4.49 nm). However, nisin and GSE treatments significantly increased the surface roughness of *L. monocytogenes*, in particular, the SSA184 strain ($P < 0.05$). The combination treatment resulted in the largest RMS roughness value (SSA184: 10.12 nm) which was almost 3 times of the respective control one.

Based on the AFM images and quantitative results, it is suggested that nisin resulted in cell morphology changes and pores formation. Therefore, we inferred that the nisin destroyed the cytoplasmic membrane by forming pores and changing cell membrane permeability. These results were supported by previous studies which proposed that the inactivation mechanism of nisin against bacteria included destroying bacterial cell membranes which led to pore formation and cell collapse (Santos et al., 2018). On the other hand, although the antimicrobial effect of GSE especially on Gram-positive bacteria have been well studied, limited studies were carried out on its action mechanism analysis (Adámez, Samino, Sánchez, & González-gómez, 2012). Kao et al. (2010) found that the GSE inactivated *S. aureus* by inhibiting enzyme activities such as dihydrofolate reductase. In addition, Zhao et al. (2020) indicated that the GSE inactivated *L. monocytogenes* by

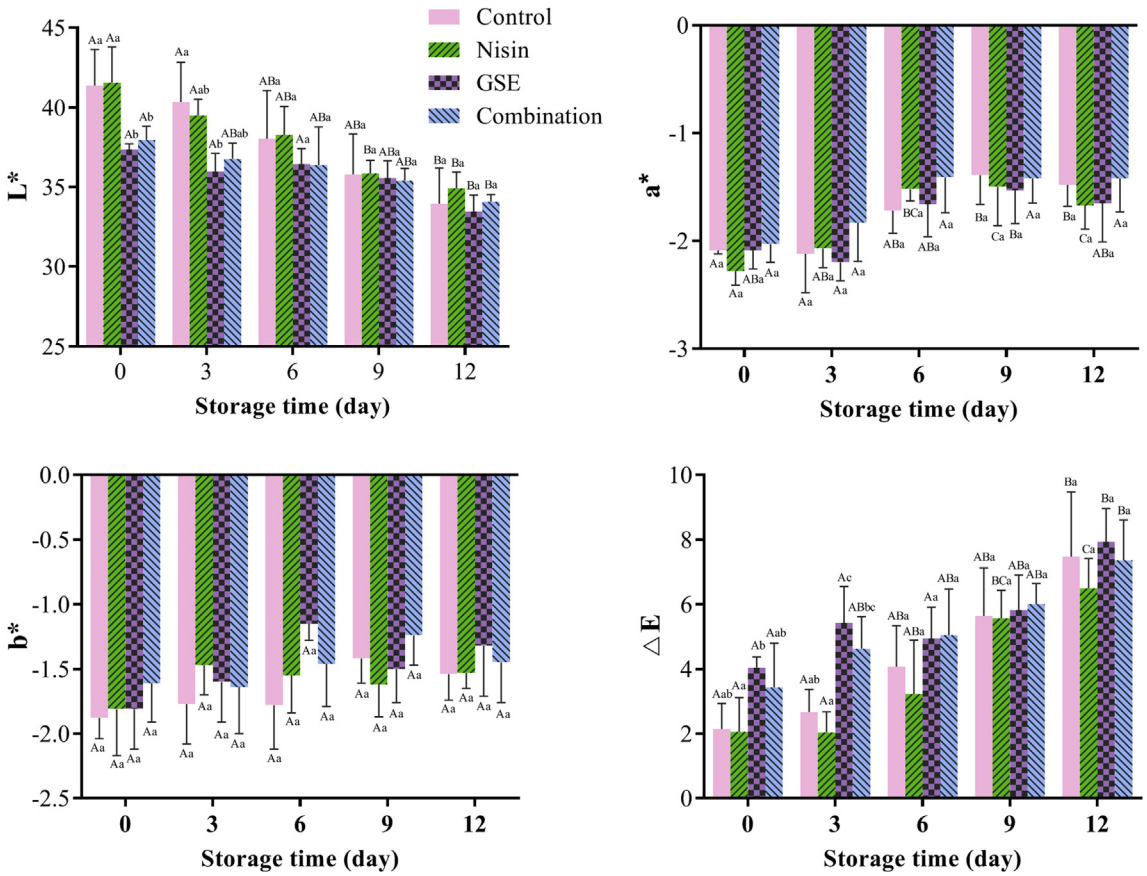

Fig. 5. Colour changes of shrimps under different treatments during storage. (A) L*; (B) a*; (C) b*; (D) overall colour difference of shrimps (ΔE). Note: Mean values with different lowercase on the same day and uppercase letters in the same group are significantly different ($P < 0.05$). (For interpretation of the references to colour in this figure legend, the reader is referred to the Web version of this article.)

inhibiting enzyme activities such as TCA cycle, energy-producing pathway and amino acid metabolism. The antimicrobial mechanism of procyanidins (primary component of GSE) has been studied in previous research. For example, disruption of cell morphology, cell permeability and cell integrity of two *E. coli* strains were observed after treatment of procyanidins from lotus seedpod (Tang, Xie, & Sun, 2017). Li et al. (2017) studied the antibacterial mechanisms of Larch bark procyanidins on *S. aureus* from the aspects of morphological structure, cell wall and membrane, essential proteins, and genetic material. The results showed that procyanidins inhibited the survival of *S. aureus* not only by destroying the cell walls and membranes but also by affecting protein synthesis and binding to DNA to form complexes. The possible mechanism of GSE and nisin might be like this: the nisin firstly destroys the structure of bacterial cell wall and changes the permeability of cell membranes, and then GSE together with nisin enters the cell and interacts with intercellular components.

3.5. Colour changes of shrimps during storage

Shrimps inoculated with *L. monocytogenes* SSA184 was chosen as a model to assess the effect of nisin and GSE on colour qualities during 12-day storage. As presented in Fig. 5, the L* value of shrimps treated with GSE only or combined GSE (day 0, within 1h after antimicrobial treatment) was significantly smaller than the control and nisin groups ($P < 0.05$), indicating that the addition of GSE darkened the shrimps. After 6 days, no significant difference on lightness was observed among four groups ($P > 0.05$). Inhibited decrease of lightness on GSE-treated shrimps suggested that GSE contributed to the lightness maintenance during storage as compared with the control and nisin groups. These results were consistent with a previous research reporting the effect of GSE on inhibiting lightness fading of meat products (Kulkarni, DeSantos, Kattamuri, Rossi, & Brewer, 2011). It is also observed that no significant changes of a* and b* values were observed among different groups during 12-day storage ($P > 0.05$). Moreover, there was no significant difference in ΔE value between control group and nisin and/or GSE treated groups after 3 days ($P > 0.05$). Generally, nisin treatment did not negatively affect colour attributes of shrimps during storage. As for GSE treatment, though colour quality was slightly affected in the beginning of storage, it provided an additional protection to colour degradation during prolonged shelf life (Kakaei & Shahbazi, 2016).

4. Conclusion

The antimicrobial effects of nisin and GSE against *L. monocytogenes* on shrimps were evaluated. Their combination yielded an enhanced and more lasting antilisterial effect than working alone. Weibull and Baranyi models satisfactorily fitted the survival and growth kinetics of *L. monocytogenes*, respectively. The combination group required the shortest time for 1 log CFU/g reduction of *L. monocytogenes* and resulted in the minimum growth at 4 °C. Furthermore, *L. monocytogenes* were visibly distorted with formed pores in the surface of cell membranes. Interestingly, the colour of shrimps was not negatively influenced during storage. In conclusion, the combined nisin and GSE could be a promising strategy for seafood industry to control the *L. monocytogenes* contamination and maintain the seafood safety.

CRediT authorship contribution statement

Xue Zhao: Conceptualization, Methodology, Investigation, Writing - original draft. **Lin Chen:** Conceptualization, Software, Investigation. **Lin Zhao:** Methodology. **Yun He:** Validation. **Hongshun Yang:** Conceptualization, Funding acquisition, Project administration, Supervision, Writing - review & editing.

Declaration of competing interest

The authors declare that they have no known competing financial interests or personal relationships that could have appeared to influence the work reported in this paper.

Acknowledgements

The work was funded by Singapore Ministry of Education Academic Research Fund Tier 1 (R-160-000-A40-114), Natural Science Foundation of Jiangsu Province (BK20181184), and an industry project (R-160-000-A21-597) from Shanghai ProfLeader Biotech Co., Ltd.

Appendix A. Supplementary data

Supplementary data to this article can be found online at https://doi.org/10.1016/j.foodcont.2020.107278.

References

Abee, T. (1995). Pore-forming bacteriocins of Gram-positive bacteria and self-protection mechanisms of producer organisms. *FEMS Microbiology Letters, 129*(1), 1–9.
Adámez, J. D., Samino, E. G., Sánchez, E. V., & González-gómez, D. (2012). *In vitro* estimation of the antibacterial activity and antioxidant capacity of aqueous extracts from grape-seeds (*Vitis vinifera* L.). *Food Control, 24*, 136–141.
Afari, G. K., & Hung, Y. (2018). A meta-analysis on the effectiveness of electrolyzed water treatments in reducing foodborne pathogens on different foods. *Food Control, 93*, 150–164.
Alejo-Armijo, A., Glibota, N., Frías, M. P., Altarejos, J., Gálvez, A., Ortega-Morente, E., et al. (2017). Antimicrobial and antibiofilm activities of procyanidins extracted from laurel wood against a selection of foodborne microorganisms. *International Journal of Food Science and Technology, 52*(3), 679–686.
Ayyash, M., Johnson, S. K., Liu, S. Q., Mesmari, N., Dahmani, S., Al Dhaheri, A. S., et al. (2019). *In vitro* investigation of bioactivities of solid-state fermented lupin, quinoa and wheat using *Lactobacillus spp*. *Food Chemistry, 275*, 50–58.
Bekhit, M., Sánchez-González, L., Messaoud, G. B., & Desobry, S. (2016). Encapsulation of *Lactococcus lactis subsp. lactis* on alginate/pectin composite microbeads: Effect of matrix composition on bacterial survival and nisin release. *Journal of Food Engineering, 180*, 1–9.
Bergmans, L., Moisiadis, P., Van Meerbeek, B., Quirynen, M., & Lambrechts, P. (2005). Microscopic observation of bacteria: Review highlighting the use of environmental SEM. *International Endodontic Journal, 38*(11), 775–788.
Bertrand, R. L. (2019). Lag phase is a dynamic, organized, adaptive, and evolvable period that prepares bacteria for cell division. *Journal of Bacteriology, 201*(7) e00697–18.
Bisha, B., Weinsetel, N., Brehm-Stecher, B. F., & Mendonca, A. (2010). Antilisterial effects of gravinol-s grape seed extract at low levels in aqueous media and its potential application as a produce wash. *Journal of Food Protection, 73*(2), 266–273.
Bordes, C., Bouarab-Chibane, L., Forquet, V., Lantéri, P., Clément, Y., et al. (2019). Antibacterial properties of polyphenols: Characterization and QSAR (quantitative structure–activity relationship) models. *Frontiers in Microbiology, 10*, 829–851.
Chen, L., Zhang, H., Liu, Q., Pang, X., Zhao, X., & Yang, H. (2019). Sanitising efficacy of lactic acid combined with low-concentration sodium hypochlorite on *Listeria innocua* in organic broccoli sprouts. *International Journal of Food Microbiology, 295*, 41–48.
Chen, L., Zhao, X., Wu, J. E., Liu, Q., Pang, X., & Yang, H. (2020). Metabolic characterization of eight *Escherichia coli* strains and acidic responses of selected strains revealed by NMR spectroscopy. *Food Microbiology, 88* 103399.
Chen, L., Zhou, Y., He, Z., Liu, Q., Lai, S., & Yang, H. (2018). Effect of exogenous ATP on the postharvest properties and pectin degradation of mung bean sprouts (*Vigna radiata*). *Food Chemistry, 251*, 9–17.
Cotter, P. D., Guinane, C. M., & Hill, C. (2002). The LisRK signal transduction system determines the sensitivity of *Listeria monocytogenes* to nisin and cephalosporins. *Antimicrobial Agents and Chemotherapy, 46*(9), 2784–2790.
Deegan, L. H., Cotter, P. D., Hill, C., & Ross, P. (2006). Bacteriocins: Biological tools for bio-preservation and shelf-life extension. *International Dairy Journal, 16*(9), 1058–1071.
Dermesonluoglu, E., Fileri, K., Orfanoudaki, A., Tsevdou, M., Tsironi, T., & Taoukis, P. (2016). Modelling the microbial spoilage and quality decay of pre-packed dandelion leaves as a function of temperature. *Journal of Food Engineering, 184*, 21–30.
Elbashir, S., Parveen, S., Schwarz, J., Rippen, T., Jahncke, M., & DePaola, A. (2018). Seafood pathogens and information on antimicrobial resistance: A review. *Food Microbiology, 70*, 85–93.
Fancello, F., Petretto, G. L., Marceddu, S., Venditti, T., Pintore, G., et al. (2020). Antimicrobial activity of gaseous *Citrus limon* var *Pompia* leaf essential oil against *Listeria monocytogenes* on *ricotta salata* cheese. *Food Microbiology,* 103386.
Gharsallaoui, A., Oulahal, N., Joly, C., & Degraeve, P. (2016). Nisin as a food preservative: Part 1: Physicochemical properties, antimicrobial activity, and main uses. *Critical Reviews in Food Science and Nutrition, 56*(8), 1262–1274.
Ghate, V., Kumar, A., Kim, M. J., Bang, W. S., Zhou, W., & Yuk, H. G. (2017). Effect of 460 nm light emitting diode illumination on survival of *Salmonella* spp. on fresh-cut

pineapples at different irradiances and temperatures. *Journal of Food Engineering, 196*, 130–138.
Gong, F., Qian, J., Chen, Y., Yao, S., Tong, J., & Guo, H. (2018). Preparation and properties of gum Arabic cross-link binding nisin microparticles. *Carbohydrate Polymers, 197*, 608–613.
Hanušová, K., Šťastná, M., Votavová, L., Klaudisová, K., Dobiáš, J., Voldřich, M., et al. (2010). Polymer films releasing nisin and/or natamycin from polyvinyldichloride lacquer coating: Nisin and natamycin migration, efficiency in cheese packaging. *Journal of Food Engineering, 99*(4), 491–496.
Haskaraca, G., Juneja, V. K., Mukhopadhyay, S., & Kolsarici, N. (2019). The effects of grapefruit seed extract on the thermal inactivation of *Listeria monocytogenes* in *sous-vide* processed döner kebabs. *Food Control, 95*, 71–76.
Ibarra-Sánchez, L. A., Van Tassell, M. L., & Miller, M. J. (2018). Antimicrobial behavior of phage endolysin PlyP100 and its synergy with nisin to control *Listeria monocytogenes* in Queso Fresco. *Food Microbiology, 72*, 128–134.
Jiang, Z., Neetoo, H., & Chen, H. (2011). Efficacy of freezing, frozen storage and edible antimicrobial coatings used in combination for control of *Listeria monocytogenes* on roasted Turkey stored at chiller temperatures. *Food Microbiology, 28*(7), 1394–1401.
Jin, T., Zhang, H., & Boyd, G. (2010). Incorporation of preservatives in polylactic acid films for inactivating *Escherichia coli* O157: H7 and extending microbiological shelf life of strawberry puree. *Journal of Food Protection, 73*(5), 812–818.
Jones, G. S., & D'Orazio, S. E. (2013). *Listeria monocytogenes*: Cultivation and laboratory maintenance. *Current Protocols in Microbiology, 31*(5) 9B.2.1–9B.2.7.
Kakaei, S., & Shahbazi, Y. (2016). Effect of chitosan-gelatin film incorporated with ethanolic red grape seed extract and *Ziziphora clinopodioides* essential oil on survival of *Listeria monocytogenes* and chemical, microbial and sensory properties of minced trout fillet. *Lebensmittel-Wissenschaft und -Technologie- Food Science and Technology, 72*, 432–438.
Kao, T., Tu, H., Chang, W., Chen, B., Shi, Y., Chang, T., et al. (2010). Grape seed extract inhibits the growth and pathogenicity of *Staphylococcus aureus* by interfering with dihydrofolate reductase activity and folate-mediated one-carbon metabolism. *International Journal of Food Microbiology, 141*, 17–27.
Kulkarni, S., DeSantos, F. A., Kattamuri, S., Rossi, S. J., & Brewer, M. S. (2011). Effect of grape seed extract on oxidative, color and sensory stability of a pre-cooked, frozen, re-heated beef sausage model system. *Meat Science, 88*(1), 139–144.
Li, X., He, C., Song, L., Li, T., Cui, S., Zhang, L., et al. (2017). Antimicrobial activity and mechanism of Larch bark procyanidins against *Staphylococcus aureus*. *Acta Biochimica et Biophysica Sinica, 49*(12), 1058–1066.
Liu, H., Pei, H., Han, Z., Feng, G., & Li, D. (2015). The antimicrobial effects and synergistic antibacterial mechanism of the combination of ε-Polylysine and nisin against *Bacillus subtilis*. *Food Control, 47*, 444–450.
Liu, Q., Tan, C. S. C., Yang, H., & Wang, S. (2017). Treatment with low-concentration acidic electrolysed water combined with mild heat to sanitise fresh organic broccoli (*Brassica oleracea*). *LWT-Food Science and Technology, 79*, 594–600.
Liu, Q., & Yang, H. (2019). Application of atomic force microscopy in food microorganisms. *Trends in Food Science & Technology, 87*, 73–83.
Morsy, M. K., Elsabagh, R., & Trinetta, V. (2018). Evaluation of novel synergistic antimicrobial activity of nisin, lysozyme, EDTA nanoparticles, and/or ZnO nanoparticles to control foodborne pathogens on minced beef. *Food Control, 92*, 249–254.
Müller-Auffermann, K., Grijalva, F., Jacob, F., & Hutzler, M. (2015). Nisin and its usage in breweries: A review and discussion. *Journal of the Institute of Brewing, 121*(3), 309–319.
Nyhan, L., Begley, M., Mutel, A., Qu, Y., Johnson, N., & Callanan, M. (2018). Predicting the combinatorial effects of water activity, pH and organic acids on *Listeria* growth in media and complex food matrices. *Food Microbiology, 74*, 75–85.
Ochoa-Velasco, C. E., Díaz-Lima, M. C., Ávila-Sosa, R., Ruiz-López, I. I., Corona-Jiménez, E., Hernández-Carranza, P., et al. (2018). Effect of UV-C light on *Lactobacillus rhamnosus, Salmonella Typhimurium*, and *Saccharomyces cerevisiae* kinetics in inoculated coconut water: Survival and residual effect. *Journal of Food Engineering, 223*, 255–261.
Okpala, C. O. R. (2015). The physicochemical changes of farm-raised Pacific white shrimp (*Litopenaeus vannamei*) as influenced by iced storage. *Food and Nutrition Sciences, 6*(10), 906–921.
Omac, B., Moreira, R. G., & Castell-Perez, E. (2018). Quantifying growth of cold-adapted *Listeria monocytogenes* and *Listeria innocua* on fresh spinach leaves at refrigeration temperatures. *Journal of Food Engineering, 224*, 17–26.
Oshima, S., Hirano, A., Kamikado, H., Nishimura, J., Kawai, Y., & Saito, T. (2014). Nisin A extends the shelf life of high-fat chilled dairy dessert, a milk-based pudding. *Journal of Applied Microbiology, 116*(5), 1218–1228.
Raeisi, M., Tabaraei, A., Hashemi, M., & Behnampour, N. (2016). Effect of sodium alginate coating incorporated with nisin, *Cinnamomum zeylanicum*, and rosemary essential oils on microbialsami quality of chicken meat and fate of *Listeria monocytogenes* during refrigeration. *International Journal of Food Microbiology, 238*, 139–145.
Rodríguez, A. C., Alcalá, E. B., Gimeno, R. G., & Cosano, G. Z. (2000). Growth modelling of *Listeria monocytogenes* in packaged fresh green asparagus. *Food Microbiology, 17*(4), 421–427.
Santos, J. C. P., Sousa, R. C. S., Otoni, C. G., Moraes, A. R. F., Souza, V. G. L., Medeiros, E. A. A., et al. (2018). Nisin and other antimicrobial peptides: Production, mechanisms of action, and application in active food packaging. *Innovative Food Science & Emerging Technologies, 48*, 179–194.
Schelegueda, L. I., Delcarlo, S. B., Gliemmo, M. F., & Campos, C. A. (2016). Effect of antimicrobial mixtures and modified atmosphere packaging on the quality of Argentine hake (*Merluccius hubbsi*) burgers. *Lebensmittel-Wissenschaft und -Technologie- Food Science and Technology, 68*, 258–264.
Semeano, A. T. S., Maffei, D. F., Palma, S., Li, R. W. C., Franco, B. D. G. M., Roque, A. C. A., et al. (2018). Tilapia fish microbial spoilage monitored by a single optical gas sensor. *Food Control, 89*, 72–76.
Shi, C., Cui, J., Yin, X., Luo, Y., & Zhou, Z. (2014). Grape seed and clove bud extracts as natural antioxidants in silver carp (*Hypophthalmichthys molitrix*) fillets during chilled storage: Effect on lipid and protein oxidation. *Food Control, 40*, 134–139.
Shi, C., Zhang, X., Zhao, X., Meng, R., Liu, Z., Chen, X., et al. (2017). Synergistic interactions of nisin in combination with cinnamaldehyde against *Staphylococcus aureus* in pasteurized milk. *Food Control, 71*, 10–16.
Sofra, C., Tsironi, T., & Taoukis, P. S. (2018). Modeling the effect of pre-treatment with nisin enriched osmotic solution on the shelf life of chilled vacuum packed tuna. *Journal of Food Engineering, 216*, 125–131.
Solomakos, N., Govaris, A., Koidis, P., & Botsoglou, N. (2008). The antimicrobial effect of thyme essential oil, nisin, and their combination against *Listeria monocytogenes* in minced beef during refrigerated storage. *Food Microbiology, 25*(1), 120–127.
Stergiou, V. A., Thomas, L. V., & Adams, M. R. (2006). Interactions of nisin with glutathione in a model protein system and meat. *Journal of Food Protection, 69*(4), 951–956.
Tabasco, R., Sánchez-patán, F., Monagas, M., Bartolomé, B., Moreno-arribas, M. V., Peláez, C., et al. (2011). Effect of grape polyphenols on lactic acid bacteria and bifidobacteria growth: Resistance and metabolism. *Food Microbiology, 28*(7), 1345–1352.
Tang, C., Xie, B., & Sun, Z. (2017). Antibacterial activity and mechanism of B-type oligomeric procyanidins from lotus seedpod on enterotoxigenic *Escherichia coli*. *Journal of Functional Foods, 38*, 454–463.
Valdivia-Nájar, C. G., Martín-Belloso, O., Giner-Seguí, J., & Soliva-Fortuny, R. (2017). Modeling the inactivation of *Listeria innocua* and *Escherichia coli* in fresh-cut tomato treated with pulsed light. *Food and Bioprocess Technology, 10*(2), 266–274.
Vongkamjan, K., Benjakul, S., Vu, H. T. K., & Vuddhakul, V. (2017). Longitudinal monitoring of *Listeria monocytogenes* and *Listeria* phages in seafood processing environments in Thailand. *Food Microbiology, 66*, 11–19.
Wu, S., Yu, P., & Flint, S. (2017). Persister cell formation of *Listeria monocytogenes* in response to natural antimicrobial agent nisin. *Food Control, 77*, 243–250.
Xu, W., Qu, W., Huang, K., Guo, F., Yang, J., Zhao, H., et al. (2007). Antibacterial effect of Grapefruit Seed Extract on food-borne pathogens and its application in the preservation of minimally processed vegetables. *Postharvest Biology and Technology, 45*, 126–133.
Yang, H., Wang, Y., Lai, S., An, H., Li, Y., & Chen, F. (2007). Application of atomic force microscopy as a nanotechnology tool in food science. *Journal of Food Science, 72*(4), R65–R75.
Ye, K., Wang, H., Zhang, X., Jiang, Y., Xu, X., & Zhou, G. (2013). Development and validation of a molecular predictive model to describe the growth of *Listeria monocytogenes* in vacuum-packaged chilled pork. *Food Control, 32*, 246–254.
Yuan, W., Lee, H. W., & Yuk, H. G. (2017). Antimicrobial efficacy of *Cinnamomum javanicum* plant extract against *Listeria monocytogenes* and its application potential with smoked salmon. *International Journal of Food Microbiology, 260*, 42–50.
Zhao, X., Chen, L., Wu, J. E., He, Y., & Yang, H. (2020). Elucidating antimicrobial mechanism of nisin and grape seed extract against *Listeria monocytogenes* in broth and on shrimp through NMR-based metabolomics approach. *International Journal of Food Microbiology, 319* 108494.
Zhao, X., Liu, Z., Li, W., Li, X., Shi, C., Meng, R., et al. (2014). *In Vitro* synergy of nisin and coenzyme Q_0 against *Staphylococcus aureus*. *Food Control, 46*, 368–373.
Zhao, X., Wu, J. E., Chen, L., & Yang, H. (2019a). Effect of vacuum impregnated fish gelatin and grape seed extract on metabolite profiles of tilapia (*Oreochromis niloticus*) fillets during storage. *Food Chemistry, 293*, 418–428.
Zhao, L., Zhao, M. Y., Phey, C. P., & Yang, H. (2019b). Efficacy of low concentration acidic electrolysed water and levulinic acid combination on fresh organic lettuce (*Lactuca sativa* Var. *Crispa* L.) and its antimicrobial mechanism. *Food Control, 101*, 241–250.
Zhao, X., Zhou, Y., Zhao, L., Chen, L., He, Y., & Yang, H. (2019c). Vacuum impregnation of fish gelatin combined with grape seed extract inhibits protein oxidation and degradation of chilled tilapia fillets. *Food Chemistry, 294*, 316–325.